2016 3rd International Conference on Information Science and Control Engineering

ICISCE

Singularity Analysis of a Novel 4-DOF Surgical Robot

Alaa Khalifa*, Mohamed Fanni§, and Abdelfatah M.Mohamed¶

*§¶Mechatronics and Robotics Engineering Dep., Egypt-Japan University of Science and Technology, School of Innovative Design Engineering, New Borg El-Arab city, Alexandria, Egypt

§On leave: Production Engineering and Mechanical Design Dep., Faculty of Engineering, Mansoura University, Egypt

¶On leave: Electrical Engineering Dep., Faculty of Engineering, Assuit University, Egypt

Email: {alaa.khalifa, mohamed.fanni, abdelfatah.mohamed}@ejust.edu.eg

***Abstract*—This paper presents the singularity analysis of a novel endoscopic surgical parallel manipulator. The 4-DOF, 2-PUU_ 2-PUS, surgical robot design has larger bending angles and workspace volume. All previous manipulators have a zero pitch and infinity pitch reciprocal screws, so it is easy to find out the singular configurations inside the workspace. On the other hand, the novel 4-DOF surgical robot (2-PUU_2-PUS) has h-pitch reciprocal screws. The known geometrical approach for reciprocal-screws could not provide all singular configurations of the novel manipulator. Geometrical/Analytical approach for reciprocal-screws based singularity analysis of 2-PUU_2-PUS is proposed. The proposed algorithm can find all singular configurations of any limited DOF parallel manipulator with h-pitch reciprocal screws. The results show the feasibility of the proposed algorithm to find all singular configurations of the 4-DOF parallel manipulator. The discovered singularity configurations shrieked greatly the singularity free workspace to one fourth the original workspace. In order to be able to work through the entire workspace, we suggest changing the topology structure of the manipulator.**

***Keywords*-Surgical robot; parallel manipulator; reciprocal screws; constraint singularity; architecture singularity**

I. Introduction

Generally, endoscopic manipulators that are in clinical use can be classified into two main categories: a flexible mechanism, usually driven by wires, and rigid mechanism manipulators. Almost all surgical commercial systems are based on flexible mechanisms which transfer the mechanical movement across the wires. There are two types of commercial systems that use flexible wire driven mechanism, the first one which is currently in clinical use is the da Vinci system which is produced by Intuitive Surgical, Inc. [1]. And the second, which was in clinical use but now stopped, is Zeus system produced by computer motion, Inc. [2]. However, the use of wire actuated type is widely spread out; it has a lot of flaws such as difficulty in the process of sterilization in endoscopic applications. Also, rupture of the wire may be occurred during the operation and the surgeon needs to complete the operation by himself. Moreover, wires may be slacked and it is required to design a mechanism to pre-tension the wires.

The second type is rigid mechanism manipulators which uses a parallel manipulator in the process of transmitting the motion to the end effector and perform the surgery. Recently, parallel mechanisms are actively participates in many medical applications because of their potential advantages compared with those of the serial. These advantages are the large payload capacity, high structural stiffness, accurate positioning, and easiness of sterilization process. An endoscopic manipulator has been developed by Rose. et al. [3]. This manipulator uses parallel kinematic mechanism, but the maximum bending angles of the manipulator is not equal in all directions due to the different design of parallel chains. This manipulator can achieve $\pm 80^o$ in one direction and $\pm 40^o$ in the perpendicular direction. However, the kinematics analysis of this mechanism is very difficult and not reported. Kobayashi et al. [4] have presented an active forceps manipulator that possess high stiffness. The drawback of this manipulator is the bending angle range which can not exceed 50^o due to limitations in the design of the forceps manipulator.

A 4-DOF parallel manipulator (2-PUU_2-PUS) was proposed [5]. The feasibility of (2-PUU_2-PUS) design is proved by computer simulations. Moreover, workspace of the bending mechanism is increased dramatically. The bending angle of this manipulator reached the limits of $\pm 90^o$ in all directions which was validated. Finally, a real model of the 4-DOF parallel manipulator is fabricated from annealed stainless steel. It is found during experimental work that the movable platform of the proposed parallel manipulator could not resist forces in some configurations. Hence, thoroughly singularity analysis is needed to discover the source of the above problem. Also, design modification of the proposed manipulator is needed to overcome this problem. The main goal of this research is to investigate the singularity problems and determine all the singular points inside the workspace.

This paper is organized as follows. In Section II, the description of the the slave surgical manipulator is briefly presented. Proposed geometrical/analytical approach for reciprocal-screws based singularity analysis of 2-PUU_2-PUS is presented in Section III. In Section IV, singular configurations of parallel surgical manipulator (2-PUU_2-PUS) are described. Finally, conclusions and future work are summarized in Section V.

978-1-5090-2535-0/16 $31.00 © 2016 IEEE
DOI 10.1109/ICISCE.2016.242

IEEE computer society

Authorized licensed use limited to: WASEDA UNIVERSITY LIBRARY. Downloaded on September 16,2020 at 13:33:15 UTC from IEEE Xplore. Restrictions apply.

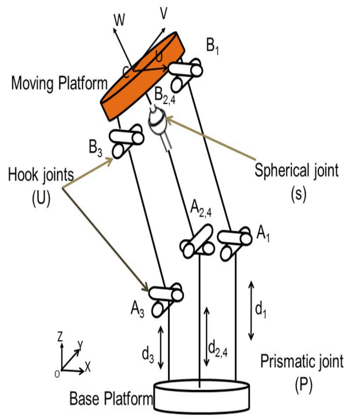

Figure 1. Schematic diagram of (2-PUU_2-PUS)

Figure 2. Real model of (2-PUU_2-PUS)

II. Slave Manipulator Description

2-PUU_2-PUS architecture is the latest implemented design of the slave surgical manipulator. The schematic diagram of the proposed endoscopic surgical manipulator (2-PUU_2-PUS) is shown in Fig. 1. To obtain larger bending angles and workspace volume, the design of 4-DOF parallel manipulator (2-PUU_2-PUS) is performed using parallel virtual chain methodology and the screw theory. This parallel mechanism consists of four limbs; two limbs are 2-PUU (each limb contains one active prismatic joint and two consecutive passive hook joints respectively); the other two limbs are 2-PUS (each limb contains one active prismatic joint, one passive hook joint and one passive spherical joint respectively). The base platform is connected to each limb by active prismatic(P) joint. The real prototype of the designed endoscopic surgical manipulator (2-PUU_2-PUS) is fabricated from annealed stainless steel as illustrated in Fig. 2.

III. Proposed Geometrical/Analytical Approach for Reciprocal-Screws Based Singularity Analysis of 2-PUU_2-PUS.

Tsai et al. [6] used the reciprocal screws to build overall square Jacobian matrix (6 * 6) for any parallel manipulator with limited DOF. A limited DOF parallel manipulator has F-DOF, considering F is between 0 and 6. It is considered that only one actuator drives each limb as we are interested in this case only. Reciprocal screws theory is applied to find the Jacobian matrix that relates the joints rate and the end-effector velocities. Overall Jacobian matrix gives information about both constraint and architecture singularities. Constraint singularities arise when the limbs of parallel manipulator with limited-DOF lose their ability to constrain the movable platform to move with the intended motion. While architecture singularities refer to the conditions for which the actuators cannot control the linear velocity of the movable platform.

All previous manipulators have a zero pitch and infinity pitch reciprocal screws, so it is easy to imagine the singular configurations inside the workspace. A zero pitch reciprocal screw means that the movable platform is constrained by pure force. While, infinity pitch reciprocal screw means that the movable platform is constrained by pure couple. On the other hand, the novel 4-DOF surgical robot (2-PUU_2-PUS) has h-pitch reciprocal screws. h-pitch reciprocal screw means that the movable platform is constrained by a combination between forces and couples. It is difficult to find out the singular configurations as h-pitch reciprocal screw depends on the configuration and changed during the operation. Hence, the known geometrical approach for reciprocal-screws could not provide all singular configurations of the novel manipulator. Geometrical/Analytical approach for reciprocal-screws based singularity analysis of 2-PUU_2-PUS is proposed. The proposed algorithm can find all singular configurations of any limited DOF parallel manipulator with h-pitch reciprocal screws. The proposed algorithm will be discussed in this section.

At the center of the fixed plate we attached a fixed frame OXYZ in which the X-axis points to the direction of OP_1. Moreover, the Z-axis is perpendicular to the plane of the base plate. Finally, Y-axis will satisfy the right hand rule. Furthermore, at the center of the mobile plate, a mobile frame CUVW with the same pose as the fixed frame is attached. Considering the first limb PUU, those fixed and mobile frames are shown in Fig. 3. The P-joint that connects the base plate to the limb is the active joint. Due to the movement of the actuators, links P_iA_i are of variable lengths d_i in the Z-direction. Links P_iA_i and A_iB_i are tied by the hook joint. Links A_iB_i are of fixed length L_i. The coordinates of the points P_i referred to the fixed base reference frame XYZ are given by:

$$P_1 = \begin{bmatrix} R \\ 0 \\ 0 \end{bmatrix}, P_2 = \begin{bmatrix} 0 \\ R \\ 0 \end{bmatrix}, P_3 = \begin{bmatrix} -R \\ 0 \\ 0 \end{bmatrix}, P_4 = \begin{bmatrix} 0 \\ -R \\ 0 \end{bmatrix} \quad (1)$$

While the coordinates of points A_i referred to the location of the first hook joints for each chain and can be calculated from:

$$A_i = P_i + \begin{bmatrix} 0, & 0, & d_i \end{bmatrix}^T \quad ,where \quad i = 1,2,3,4 \quad (2)$$

In the following subsections, we will find the reciprocal screws with the actuators locked and without locking the actuators for all limbs.

A. First and Third Limbs

Like the first limb, the third limb connects the fixed plate to the movable platform by a prismatic joint followed by two hook joints (PUU). The prismatic joint is driven by a linear actuator. In this subsection, $i = 1$ for the first limb and

Authorized licensed use limited to: WASEDA UNIVERSITY LIBRARY. Downloaded on September 16,2020 at 13:33:15 UTC from IEEE Xplore. Restrictions apply.

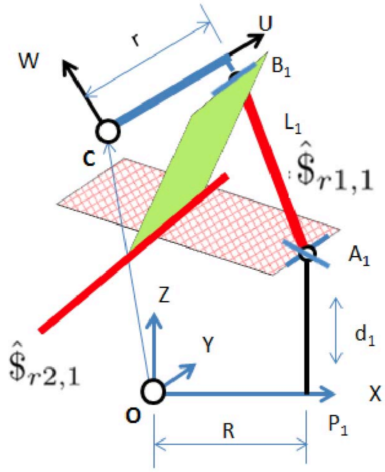

Figure 3. Reciprocal screws of first chain PUU

$i = 3$ for the third limb. Let $s_{j,i}$ be a unit vector along the j^{th} joint axis of the i^{th} limb. A unit vector associated with all joints axis in the i^{th} limb is driven. The fixed frame OXYZ is chosen to be the reference frame at which all the screws are expressed. For the prismatic joint, the pitch of the screw will be infinity and the unit screw is reduced to: $\hat{\$}_{1,i} = \begin{bmatrix} [0]_{3*1} \\ s_{1,i} \end{bmatrix}$. For the revolute joint, the pitch of the screw will be zero and the unit screw is calculated as: $\hat{\$}_{k,i} = \begin{bmatrix} s_{k,i} \\ s_{0k,i} \times s_{k,i} \end{bmatrix}$ where $k = 2,3,4,5$. Moreover, $s_{0k,i}$ is the position vector of a point laying on the screw axis and it is founded to be: $s_{02,i} = s_{03,i} = A_i$ and $s_{04,i} = s_{05,i} = B_i$. The position of the second hook joint in the i^{th} limb is symbolized by B_i.

With the actuator locked, the connectivity of the first and third limb is equal to 4. The reciprocal screws for these limbs which is reciprocal to all the passive joint screws form a 2-system. One screw, $\hat{\$}_{r1,i}$, can be readily identified as a zero pitch screw along the line passing through the center of the two hook joints. The second screw, $\hat{\$}_{r2,i}$, which is also reciprocal to all the passive joint screws can be readily identified as a zero pitch screw along the intersection line of two planes. The first plane contains the two axes of the first hook joint and the second plane contains the two axes of the second hook joint as shown in Fig. 3. The analytical part is performed by providing formulas for all joints axes, planes that contains the two axes of all hook joints, and intersection line between the planes. Finally, we get the following formulas for the reciprocal screws:

$$\hat{\$}_{r1,1} = \begin{bmatrix} \sin(\alpha_1)\cos(\beta_1) \\ -\sin(\beta_1) \\ \cos(\alpha_1)\cos(\beta_1) \\ d_1 \sin(\beta_1) \\ d_1 \sin(\alpha_1)\cos(\beta_1) - R\cos(\alpha_1)\cos(\beta_1) \\ -R\sin(\beta_1) \end{bmatrix} \quad (3)$$

$$\hat{\$}_{r2,1} = \begin{bmatrix} -\cos(\alpha_1) \\ 0 \\ \sin(\alpha_1) \\ -L_1 \sin(\alpha_1)\cos(\gamma_1)/\sin(\beta_1+\gamma_1) \\ -d_1\cos(\alpha_1) - R\sin(\alpha_1) \\ -L_1\cos(\alpha_1)\cos(\gamma_1)/\sin(\beta_1+\gamma_1) \end{bmatrix} \quad (4)$$

$$\hat{\$}_{r1,3} = \begin{bmatrix} \sin(\alpha_3)\cos(\beta_3) \\ -\sin(\beta_3) \\ \cos(\alpha_3)\cos(\beta_3) \\ d_3 \sin(\beta_3) \\ d_3 \sin(\alpha_3)\cos(\beta_3) + R\cos(\alpha_3)\cos(\beta_3) \\ R\sin(\beta_3) \end{bmatrix} \quad (5)$$

$$\hat{\$}_{r2,3} = \begin{bmatrix} -\cos(\alpha_3) \\ 0 \\ \sin(\alpha_3) \\ -L_3 \sin(\alpha_3)\cos(\gamma_3)/\sin(\beta_3+\gamma_3) \\ -d_3\cos(\alpha_3) + R\sin(\alpha_3) \\ -L_3\cos(\alpha_3)\cos(\gamma_3)/\sin(\beta_3+\gamma_3) \end{bmatrix} \quad (6)$$

Where α_i and β_i are the two angels of the first hook joint in the i^{th} limb. γ_i and δ_i are the two angels of the second hook joint in the i^{th} limb.

Without locking the prismatic joint, The connectivity of the first and third limb is equal to 5. Hence, the reciprocal screws for these limbs form a 1-system which is a screw that is a reciprocal to all the joint screws of the first and third limb respectively. This reciprocal screw ,$\hat{\$}_{rt,i}$, is a linear combination between $s_{r1,i}$ and $s_{r2,i}$ which must satisfy the condition to be a reciprocal with the prismatic joint screw. After performing the analytical part, we get the following formulas for the reciprocal screws and their pitch:

$$\hat{\$}_{rt,1} = \begin{bmatrix} \dfrac{-1}{\cos(\alpha_1)\sqrt{\frac{\cos^2(\alpha_1)\cos^2(\beta_1)-\cos^2(\alpha_1)+1}{\cos^2(\alpha_1)\cos^2(\beta_1)}}} \\ \dfrac{\sin(\alpha_1)\sin(\beta_1)}{\cos(\alpha_1)\cos(\beta_1)\sqrt{\frac{\sin^2(\alpha_1)}{\cos^2(\alpha_1)\cos^2(\beta_1)}+1}} \\ 0 \\ \dfrac{-\sin(\alpha_1)[d_1\sin(\beta_1+\gamma_1)\sin(\beta_1)+L_1\cos(\alpha_1)\cos(\beta_1)\cos(\gamma_1)]}{\sin(\beta_1+\gamma_1)\cos(\alpha_1)\cos(\beta_1)\sqrt{\frac{\sin^2(\alpha_1)}{\cos^2(\alpha_1)\cos^2(\beta_1)}+1}} \\ \dfrac{-d_1}{\cos(\alpha_1)\sqrt{\frac{\cos^2(\alpha_1)\cos^2(\beta_1)-\cos^2(\alpha_1)+1}{\cos^2(\alpha_1)\cos^2(\beta_1)}}} \\ \dfrac{-[L_1\cos^2(\alpha_1)\cos(\beta_1)\cos(\gamma_1)-R\sin(\beta_1+\gamma_1)\sin(\alpha_1)\sin(\beta_1)]}{\cos(\beta_1+\gamma_1)\cos(\alpha_1)\cos(\beta_1)\sqrt{\frac{\sin^2(\alpha_1)}{\cos^2(\alpha_1)\cos^2(\beta_1)}+1}} \end{bmatrix} \quad (7)$$

$$\lambda_1 = \frac{L_1\cos(\alpha_1)\cos^2(\beta_1)\cos(\gamma_1)\sin(\alpha_1)}{\sin(\beta_1+\gamma_1)[\cos^2(\alpha_1)\cos^2(\beta_1)-\cos^2(\alpha_1)+1]} \quad (8)$$

Authorized licensed use limited to: WASEDA UNIVERSITY LIBRARY. Downloaded on September 16,2020 at 13:33:15 UTC from IEEE Xplore. Restrictions apply.

$$\hat{\$}_{rt,3} = \begin{bmatrix} \frac{-1}{\cos(\alpha_3)\sqrt{\frac{\cos^2(\alpha_3)\cos^2(\beta_3)-\cos^2(\alpha_3)+1}{\cos^2(\alpha_3)\cos^2(\beta_3)}}} \\ \frac{\sin(\alpha_3)\sin(\beta_3)}{\cos(\alpha_3)\cos(\beta_3)\sqrt{\frac{\sin^2(\alpha_3)}{\cos^2(\alpha_3)\cos^2(\beta_3)}+1}} \\ 0 \\ \frac{-\sin(\alpha_3)[d_3\sin(\beta_3+\gamma_3)\sin(\beta_3)+L_3\cos(\alpha_3)\cos(\beta_3)\cos(\gamma_3)]}{\sin(\beta_3+\gamma_3)\cos(\alpha_3)\cos(\beta_3)\sqrt{\frac{\sin^2(\alpha_3)}{\cos^2(\alpha_3)\cos^2(\beta_3)}+1}} \\ \frac{-d_3}{\cos(\alpha_3)\sqrt{\frac{\cos^2(\alpha_3)\cos^2(\beta_3)-\cos^2(\alpha_3)+1}{\cos^2(\alpha_3)\cos^2(\beta_3)}}} \\ \frac{-[L_3\cos^2(\alpha_3)\cos(\beta_3)\cos(\gamma_3)+R\sin(\beta_3+\gamma_3)\sin(\alpha_3)\sin(\beta_3)]}{\cos(\beta_3+\gamma_3)\cos(\alpha_3)\cos(\beta_3)\sqrt{\frac{\sin^2(\alpha_3)}{\cos^2(\alpha_3)\cos^2(\beta_3)}+1}} \end{bmatrix} \quad (9)$$

$$\lambda_3 = \frac{L_3\cos(\alpha_3)\cos^2(\beta_3)\cos(\gamma_3)\sin(\alpha_3)}{\sin(\beta_3+\gamma_3)[\cos^2(\alpha_3)\cos^2(\beta_3)-\cos^2(\alpha_3)+1]} \quad (10)$$

where λ_i is the pitch of the reciprocal screw. It is clear that the pitch of the reciprocal screw λ_i depends on the configuration as it is a function of the angels of the two hook joints existed in i^{th} limb.

B. Second and Fourth Limbs

Like the Fourth limb, second limb connects the fixed base to the moving platform by a prismatic joint followed by a hook joint and another spherical joint (PUS). The prismatic joint is driven by a linear actuator. In this subsection, $i = 2$ for the second limb and $i = 4$ for the fourth limb. With the actuator locked, the reciprocal screws for this limb form a 1-system. This screw, $\hat{\$}_{r1,i}$, which is reciprocal to all the passive joint screws of the i^{th} limb can be readily identified as a zero pitch screw along the line passing through the center of the hook and spherical joints. After performing the analytical part, we get the following formulas for the reciprocal screws:

$$\hat{\$}_{r1,2} = \begin{bmatrix} \sin(\beta_2) \\ -\sin(\alpha_2)\cos(\beta_2) \\ \cos(\alpha_2)\cos(\beta_2) \\ R\cos(\alpha_2)\cos(\beta_2)+d_2\sin(\alpha_2)\cos(\beta_2) \\ d_2\sin(\beta_2) \\ -R\sin(\beta_2) \end{bmatrix} \quad (11)$$

$$\hat{\$}_{r1,4} = \begin{bmatrix} \sin(\beta_4) \\ -\sin(\alpha_4)\cos(\beta_4) \\ \cos(\alpha_4)\cos(\beta_4) \\ -R\cos(\alpha_4)\cos(\beta_4)+d_4\sin(\alpha_4)\cos(\beta_4) \\ d_4\sin(\beta_4) \\ R\sin(\beta_4) \end{bmatrix} \quad (12)$$

Where α_i and β_i are the two angels of the first hook joint in the i^{th} limb. γ_i, δ_i , and σ_i are the three angels of the spherical joint in the i^{th} limb.

Without locking the active prismatic joint, The connectivity of the second and fourth limb is equal to 6. Hence, no screw could be identified to be a reciprocal to all the joint screws of these limbs.

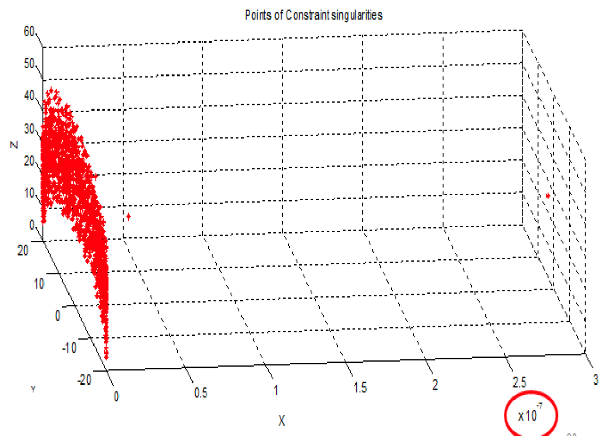

Figure 4. Points satisfy first constraint singularities condition

IV. Singular Configurations of Parallel Surgical Manipulator(2-PUU_2-PUS)

A. Constraint singularities

Constraint singularities arise when the Jacobian of constraints Jc loses its rank. These singularities will occur when $\hat{\$}^T_{rt,1}$ and $\hat{\$}^T_{rt,3}$ become linearly dependent (LD). The following states present the conditions for Constraint singularities.

(1) when $\alpha_1 = \alpha_3 = 0$ && $\beta_1 = \beta_3 = \beta$ && $\gamma_1 = \gamma_3 = \gamma$ && $d_1 = d_3 = d$

$$\hat{\$}_{rt,1} = \hat{\$}_{rt,3} = \begin{bmatrix} -1, & 0, & 0, & 0, & -d, & \frac{-L\cos(\gamma)}{\sin(\beta+\gamma)} \end{bmatrix}^T \quad (13)$$

A search for points inside the workspace and satisfy this condition is achieved. It is founded that all the points in the YZ plane can satisfy this condition as shown in Fig. 4. Hence, Constraint singularity configurations occur when the center of the movable platform lays on the YZ orthogonal plane.

(2) when $\alpha_1 = \alpha_3 = \alpha$ && $\beta_1 = \beta_3 = 0$ && $\gamma_1 = \gamma_3 = \gamma$ && $d_1 = d_3 = d$

$$\hat{\$}_{rt,1} = \hat{\$}_{rt,3} = \begin{bmatrix} -1, & 0, & 0, & \phi\sin\alpha, & -d, & \phi\cos\alpha \end{bmatrix}^T \quad (14)$$

where $\phi = \frac{-L\cos(\gamma)}{\sin(\gamma)\sqrt{\frac{1}{\cos^2(\alpha)}}}$. It is found that constraint singularity configurations occur when the center of the movable platform lays on the XZ orthogonal plane as shown in Fig. 5.

(3) when $\alpha_1 = \alpha_3 = \alpha$ && $\beta_1 = \beta_3 = \beta$ && $\gamma_1 = \gamma_3 = \gamma$ && $d_1 = d_3 = d$ && $\beta + \gamma = 0$

After searching for points inside the workspace and satisfy this condition, it is found that this condition will not occur unless $d_1 = d_2 = d_3 = d_4$.

From the above three states, we discovered that singularity configurations occur when the center of the movable platform lays on two orthogonal planes. These planes are

Authorized licensed use limited to: WASEDA UNIVERSITY LIBRARY. Downloaded on September 16,2020 at 13:33:15 UTC from IEEE Xplore. Restrictions apply.

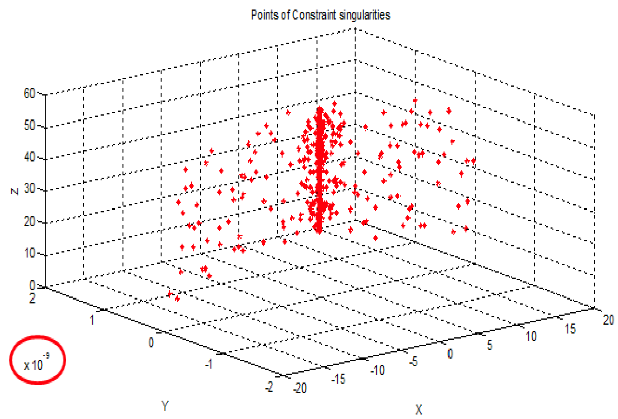

Figure 5. Points satisfy second constraint singularities condition

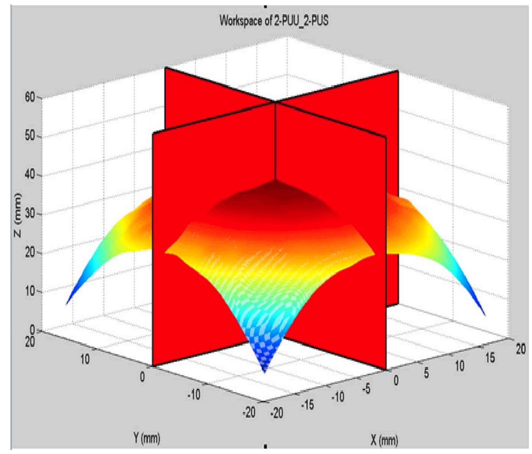

Figure 6. Workspace of 2-PUU_2-PUS with singular planes

parallel to the axes of the prismatic joints and each plane contains the axes of two opposite prismatic joints and passing through the center of the fixed base. These orthogonal planes divide the workspace into four equal parts as shown in Fig. 6. Thus, the singularity free workspace is one fourth the original workspace.

B. Architecture singularities

Architecture singularities occur when det(J)=0 but J_c has a full rank of 2. These singularities will occur when two or more of reciprocal screws from $\hat{\$}_{r1,1}$, $\hat{\$}_{r1,2}$, $\hat{\$}_{r1,3}$ and $\hat{\$}_{r1,4}$ become linearly dependent (LD). The following states present the conditions for actuation singularities.

(1) when $\alpha_1 = \alpha_3 = \pi/2$ && $\beta_1 = \beta_3 = 0$ && $d_1 = d_3 = d$

$$\hat{\$}_{r1,1} = \hat{\$}_{r1,3} = \begin{bmatrix} 1, & 0, & 0, & 0, & d, & 0 \end{bmatrix}^T \quad (15)$$

(2) when $\alpha_2 = \alpha_4 = \pi/2$ && $\beta_2 = \beta_4 = 0$ && $d_2 = d_4 = d$

$$\hat{\$}_{r1,2} = \hat{\$}_{r1,4} = \begin{bmatrix} 0, & -1, & 0, & d, & 0, & 0 \end{bmatrix}^T \quad (16)$$

From the above two states, we discovered that Architecture singularities occur when links A_iB_i are perpendicular to the prismatic joints axis which donated as P_iA_i links. So, the bending angle could not be greater than $\pm 90^o$ which is acceptable in surgical applications.

V. Conclusions

Geometrical/Analytical approach for reciprocal-screws based singularity analysis is proposed to investigate the singularity problems of any limited DOF parallel manipulator. This proposed algorithm is used to find all singular configurations inside the workspace of 2-PUU_2-PUS which has h-pitch reciprocal screws. The discovered singularity configurations of 2-PUU_2-PUS occur when the center of the movable platform lays on two orthogonal planes. These planes are parallel to the axes of the prismatic joints and each plane contains the axes of two opposite prismatic joints and passing through the center of the fixed base. These orthogonal planes divide the workspace into four equal parts. Thus, the singularity free workspace is one fourth the original workspace. As a future work, design modifications of the proposed manipulator is needed to move across the singularity planes and retain the original workspace.

Acknowledgment

The first author is supported by a scholarship from the Mission Department, Ministry of Higher Education of the Government of Egypt which is gratefully acknowledged. Our sincere thanks to Egypt-Japan University of Science and Technology (E-JUST) for guidance and support.

References

[1] G. Guthart and J. Salisbury, "The Intuitive Telesurgery System: Overview and Application," in Proc. IEEE Int. Conf. Robot. Autom., San Francisco, CA, pp. 618-621, 2000.

[2] P. Berkelman and J. Ma, "A Compact Modular Teleoperated Robotic System for Laparoscopic Surgery," in International Journal of Robotics Research, pp. 1198-1215, Sep., 2009.

[3] A. Rose, H.F. Schlaak "A Parallel Kinematic Mechanism for Highly Flexible Laparoscopic Instruments," IFMBE Proceedings vol. 22, pp. 903-906, 2008.

[4] Y. Kobayashi, S. Chiyoda, K. Watabe, M. Okada, and Y. Nakamura, "Small Occupancy Robotic Mechanisms for Endoscopic Surgery," in Proc. Int. Conf. Med. Comput.-Assist. Interv., pp. 75-82, 2002.

[5] Ibrahim, Khalil, et al. "Development of a new 4-DOF endoscopic parallel manipulator based on screw theory for laparoscopic surgery." Mechatronics 28 (2015): 4-17.

[6] Joshi, Sameer A., and Lung-Wen Tsai. "Jacobian analysis of limited-DOF parallel manipulators." ASME 2002 International design engineering technical conferences and computers and information in engineering conference. American Society of Mechanical Engineers, 2002.

Authorized licensed use limited to: WASEDA UNIVERSITY LIBRARY. Downloaded on September 16,2020 at 13:33:15 UTC from IEEE Xplore. Restrictions apply.